Nanometer emittance ultralow charge beams from rf photoinjectors

R.K. Li, K.G. Roberts, C.M. Scoby, H. To and P. Musumeci

PRST-Accel. Beams 15, 090702 (2012)

(Received 19 June 2012; published 11 September 2012)

Martin Khojoyan

PITZ Physics Seminar

12.03.2013

HELMHOLTZ ASSOCIATION

DESY

Content

- Introduction
- Simplified envelope equation model and simulation
- Creation of cigar like shaped uniformly filled ellipsoid beams
- Measurement of ultralow emittance
- Outlook and conclusions

Introduction

Possibilities for e-beams with charges lower or equal to 1pC:

- Ultralow transverse emittances (<0.1 mm mrad) [1]
- High resolution ultrafast relativistic electron diffraction and microscopy [2-4]
- Drivers for sub-fs high gain free-electron laser amplifiers (single spike lasing) [5-7]
- Suitable for external injection into laser-based high gradient acceleration structures [8,9]

In this paper authors describe the possibility of creation of uniformly filled ellipsoidal beams relying on strong space charge driven transverse expansion which is similar to blow-out (longitudinal beam expansion) regime but has an advantage of minimized thermal emittance contribution on the beam emittance.

Simplified envelope equation model and simulation

- Consider the space charge dominated transverse expansion of a beam slice with current I and initial spot size σ_0
- In the space charge dominated regime, one can neglect the emittance contribution term inside the envelope equation

$$\sigma_x'' + k_\beta^2 \sigma_x = \frac{I}{2 I_A \gamma^3 \sigma_x} \quad \rightarrow \text{ Simplified envelope equation}$$

$I_A = 17kA$ - Alfven current

k_β^2 - represents the focusing system

To stress that each slice can have different current and transverse size

It can be verified by particle tracking simulations, that $\sigma_x(\xi) \sim I(\xi)^{1/2}$

$J(\xi) \propto I(\xi)/\sigma_x(\xi)^2$ → Final current density independent of longitudinal coordinate inside the bunch

Simplified envelope equation model and simulation

By choosing the input current profile (shaping temporal profile of the laser on the cathode) to be parabolic, the beam edge will be well described by the equation of ellipse.

$$I(\xi) = I_0\left[1-\left(\xi/L\right)^2\right]$$

GPT simulations confirm, that cigarlike shaped beam (longitudinal size >> transverse size) with a parabolic current profile evolves into a nearly ideal uniformly filled ellipsoid distribution due to strong transverse expansion.

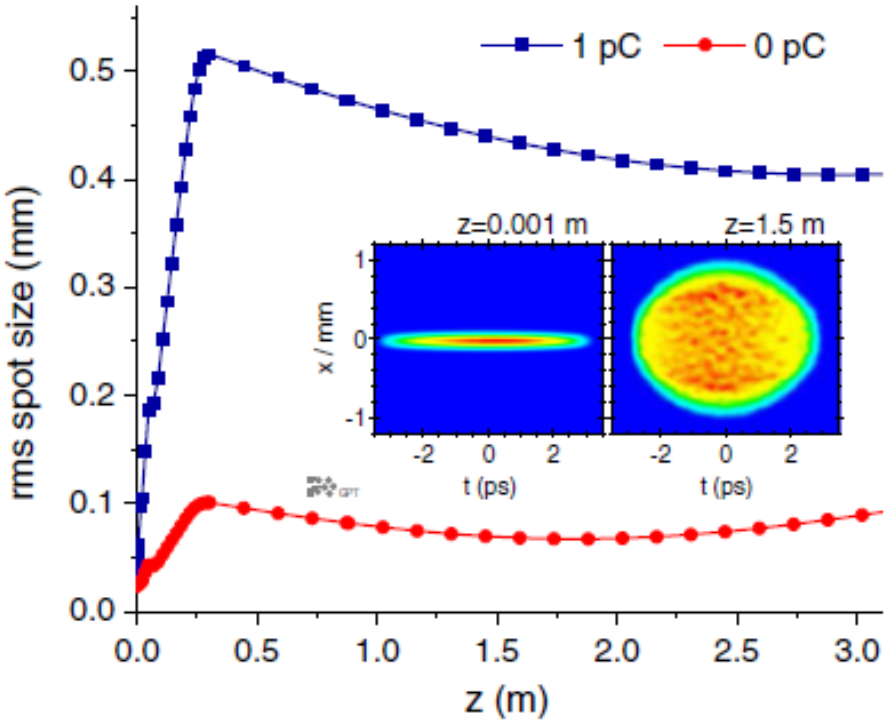

FIG. 1. GPT simulations of cigar beam dynamics in rf photoinjectors: transverse beam sizes along the Pegasus beam line for 1 pC and 0 pC (space charge effects switched off). The simulation parameters match the experimental ones reported in Table I. With proper initial conditions, the space charge dominated expansion leads to the creation of a nearly ideal uniformly filled ellipsoidal distribution (inset).

Creation of cigarlike shaped uniformly filled ellipsoid beams

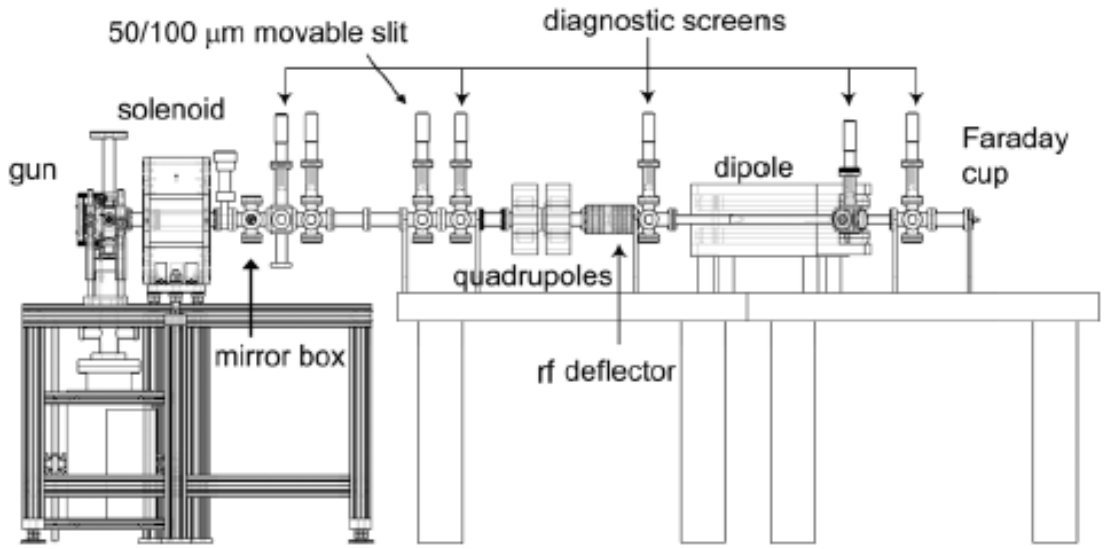

Fig.I. Layout of UCLA Pegasus photoinjector.

- 2.856 GHz, 1.6 cell RF gun
- E-beam is strongly focused (by solenoids) to a distance of ~0.75m from the cathode
- 9.6 GHz deflecting cavity is located at 1.5m after the gun

TABLE I. Pegasus photoinjector parameters for the transverse space charge dominated expansion regime.

Beam total energy	3.5 MeV
Peak field at the cathode	70 MV/m
Injection phase	30 deg
Beam charge	1 pC
Laser spot size (rms)	30 μm
Laser pulse length (rms)	1.8 ps
Bunch length at rf deflector (rms)	1.6 ps
Normalized emittance	40 nm

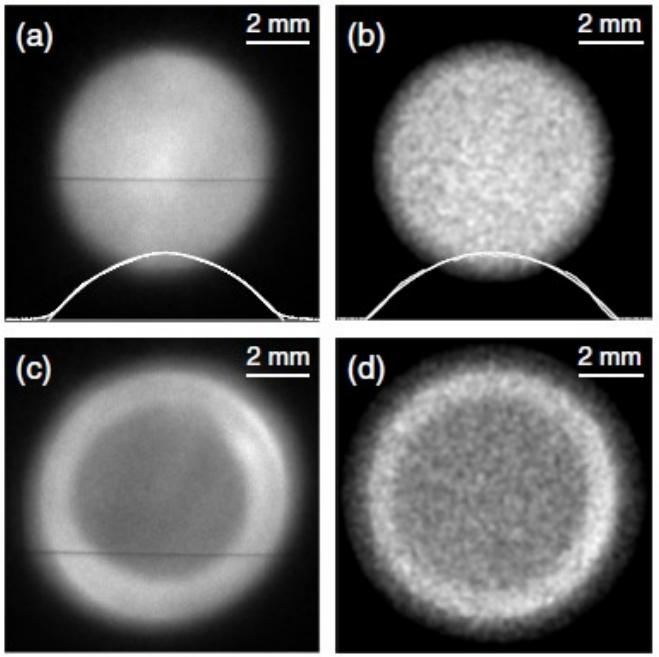

FIG. 2. Measured transverse beam profiles at $z = 3.0$ m from the cathode for (a) a stretched laser pulse and (c) a short laser pulse on the cathode. Corresponding GPT simulation results are shown in (b) and (d). The projection of the beam profiles in (a) and (b) onto one axis (dashed line) are also shown together with the parabolic fitting (solid line).

Creation of cigarlike shaped uniformly filled ellipsoid beams

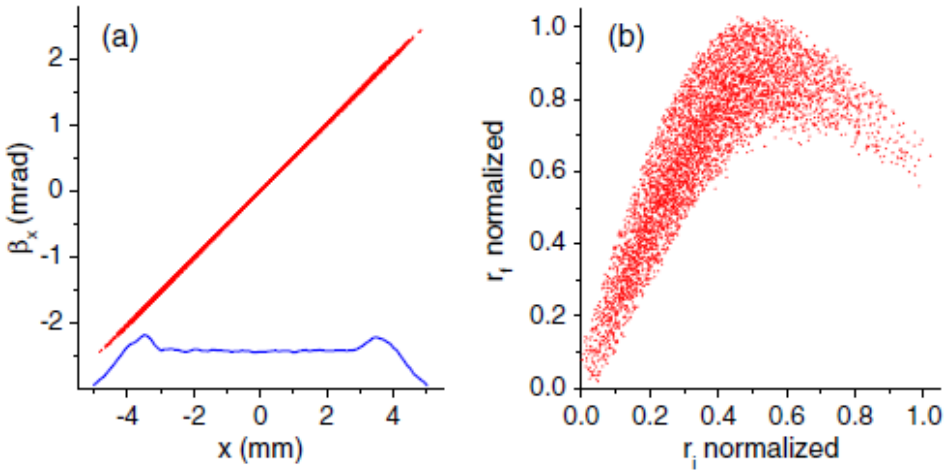

FIG. 3. (a) The transverse phase space $x - \beta_x$ of the beam when the UV stretcher was off and the laser pulse short at the cathode. The density profile along x axis is also shown (blue line). (b) The correlation between the initial transverse positions r_i at the cathode and the final positions r_f on the screen.

When the beam is short (65fs rms) at the cathode there is a strong coupling between transverse and longitudinal expansions and simplified model of beam evolution is no longer valid.

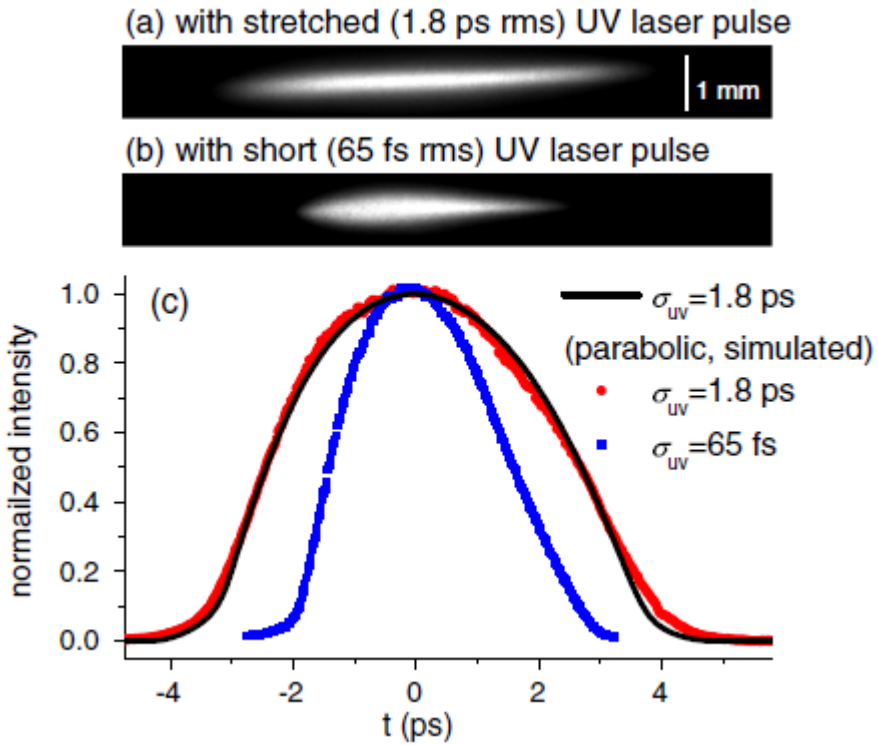

FIG. 4. Beam profiles on a transverse screen after streaked by an rf deflecting cavity when the UV laser pulse is (a) stretched to 1.8 ps rms, and (b) an ultrashort 65 fs rms distribution. Their projections onto the $t(z)$ axis are shown in (c) together with the GPT simulation result (black solid line) for an ideal 1.8 ps rms parabolic UV laser pulse.

Measurement of ultralow emittance

Simulations predict sub-100 nm emittance for such low charges. However it is a big challenge to measure such low emittances. It demands a revision of the beam optics, pepper-pot design, detection efficiency and spatial resolution of the beam profile detector.

> New high efficiency detector system developed at UCLA

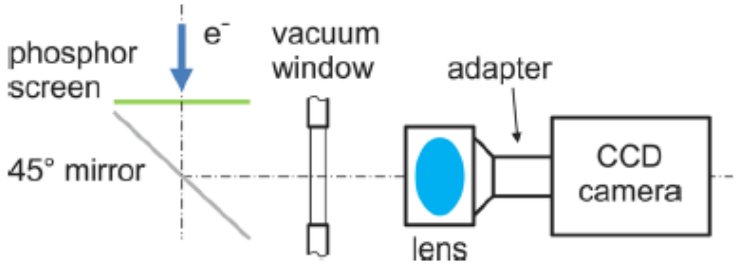

FIG. 1. (Color online) Schematic of the phosphor screen, lens-coupling optics, and CCD camera configuration.

Single MeV electron detection capacity using:

High yield (1000 photons per -e) phosphor screen

High efficiency light collection optics

Electron multiplying CCD camera (EMCCD)

Detector system was calibrated with a relativistic beam of 1.6 MeV and about 1 pC beam charge

Measurement of ultralow emittance

- Variation of pepper-pot technique → transmission electron microscopy (TEM) grid was chosen as sampling target

200 mesh copper grid (pitch size of 125 um) consisting of perpendicular copper bars that are 32 um wide and 20 um thickness was used in measurements

~50% of the electrons in the beam propagate through the grid. All other electrons will be scattered with a broad angular distribution which according to Monte Carlo simulations is outside of 2.5 mrad cone of the beamline axis.

By analyzing the position, width and height of each edge in the shadow image, one can reconstruct the trace space and emittance value at grid position

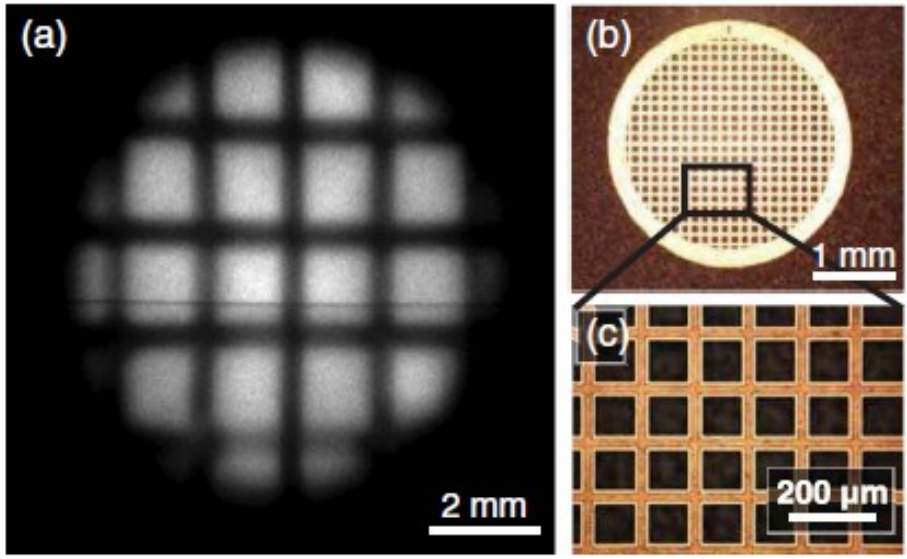

FIG. 5. (a) Electron beam shadow image on the detector screen 2.1 m after the TEM grid. The image of the grid appears magnified by a factor of 12.8. (b), (c) Optical microscope images of the 200 mesh TEM grid.

Measurement of ultralow emittance

- Variation of pepper-pot technique → transmission electron microscopy (TEM) grid

Strength of the emittance compensation solenoid tuned to have sharp beam focus at ~20 cm before the grid.

Observation screen at 2.1 m after grid

For large emittance beams divergence induced increase in beamlet image is usually much larger than the projection of the hole itself. For ultralow emittance beams this ratio can be different.

$$g(x) \propto \mathrm{erf}\left(\frac{x + Ma/2}{\sqrt{2}L\sigma_{x'}}\right) - \mathrm{erf}\left(\frac{x - Ma/2}{\sqrt{2}L\sigma_{x'}}\right)$$

σ'_x - Rms width of the beamlet

L - Distance from grid to screen

$M = 1 + L/L_0$ - Magnification of shadow image

a - Bar width

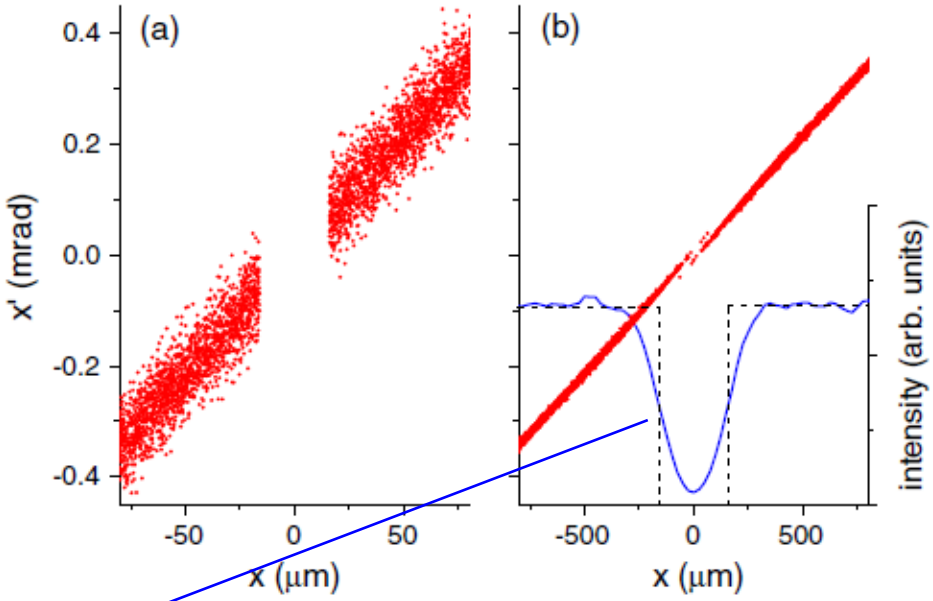

FIG. 6. Zoomed in snapshots of the $x - x'$ trace space of the beam (a) just blocked by a 32 μm grid bar and (b) at the beam profile screen 2.1 m after the grid. In (a) the beam has a uniform density along x and a Gaussian distribution in x' with an rms size of 40 μrad. The slope of the $x - x'$ band magnifies the bar image by a factor of 10. In the inset of (b) we show the shadow image of the grid bar by an ideal point source (dashed black) and the density profile of a realistic beam (solid blue).

Measurement of ultralow emittance

- Variation of pepper-pot technique → transmission electron microscopy (TEM) grid

$Ma \geq 4L\sigma'_x$ - to minimize the overlap of the signal from two nearby edges

$d > a$ - for all commercial TEM grids (where d is the grid opening, a is the bar width), so that cross talking between two adjacent bars is avoided

$\sigma_{psf} << L\sigma'_x$ Condition for spatial resolution of the beam profile detector to resolve small beam divergence (psf - point spread function)

TEM grid method has an advantage that much larger portion of electrons is transmitted

Besides extracting separate emittance values for x and y planes, the shadow image contains information about $x - p_y$ correlation (90^0 deviation of crossing bars)

Measurement of ultralow emittance

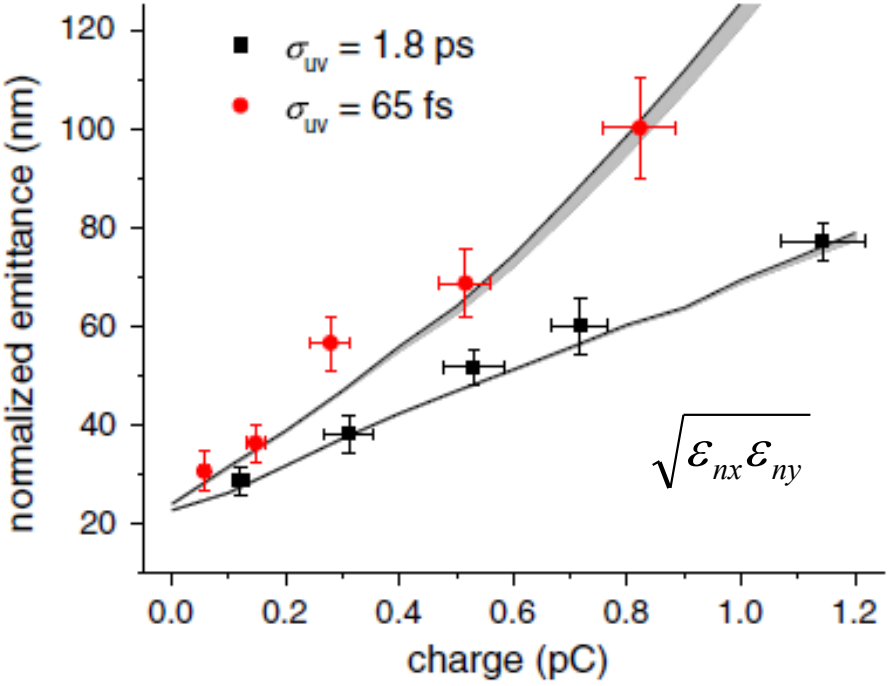

FIG. 7. Measured normalized emittance of beams when the UV laser was stretched to a 1.8 ps rms parabolic longitudinal profile (black square) and was ultrashort at 65 fs rms (red circle). The error bars indicate the statistics over 20 shots. Simulation results for both cases are also shown.

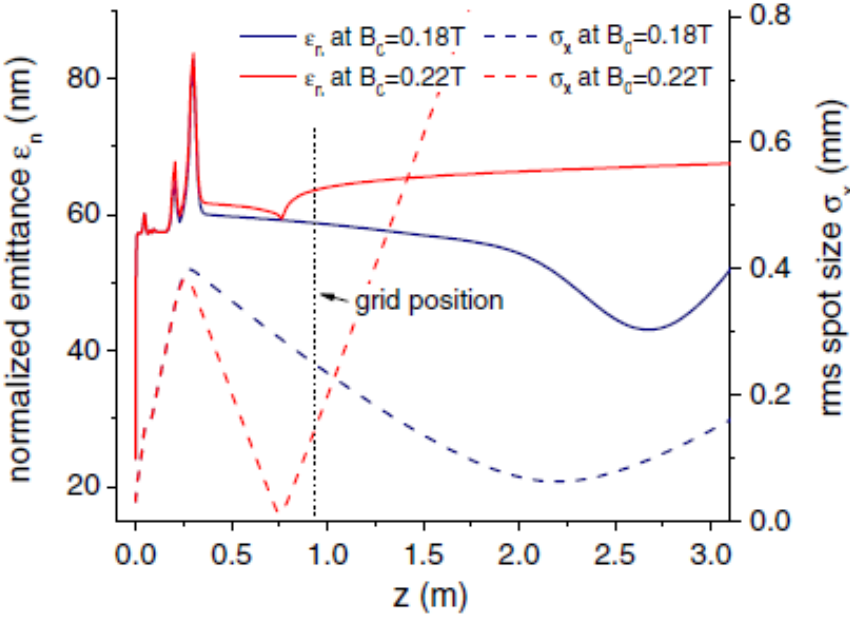

FIG. 8. Comparison of the emittance (solid lines) and spot size (dashed lines) along the beam line for the "optimal emittance mode" ($B_0 = 0.18$ T) and the "emittance measurement mode" ($B_0 = 0.22$ T). The solenoid strength is tuned to deliver the minimum emittance in the first mode and focus strongly to provide suitable M for emittance measurement using the grid method in the later mode, respectively.

In both cases laser spot size (rms) on cathode was 30 um and measurement indicates a thermal emittance level of (0.8 mm mrad)/mm rms

Simulation of ultralow emittance

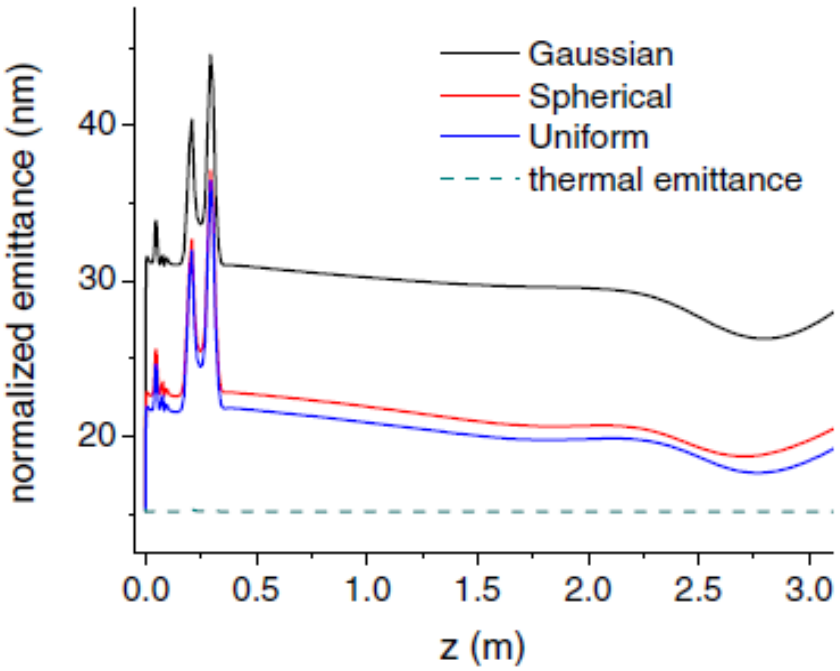

FIG. 9. Comparison of the optimal emittance for Gaussian, spherical, and uniform initial transverse distributions from the cathode (all have 20 μm rms spot sizes) for a gun gradient of 120 MV/m. For the Gaussian profile the nonlinear transverse space charge forces at the beam edge lead to slice emittance growth. For spherical and uniform cases the transverse space charge forces are more linear and the compensated projected emittance is closer to the thermal emittance level. In the later cases 1 pC, sub-20 nm beams are generated.

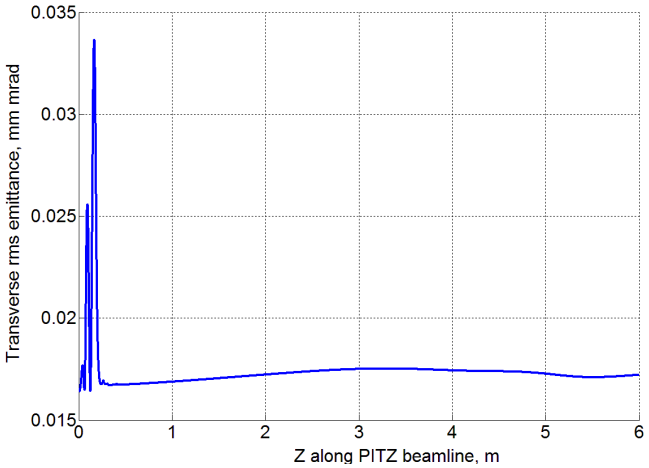

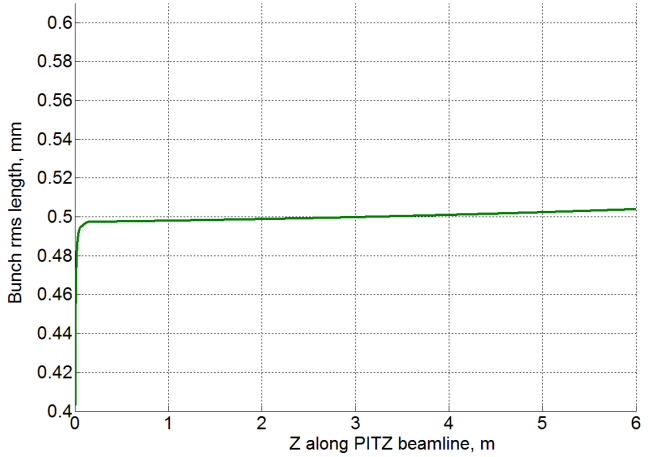

Transverse emittance and bunch length along the PITZ beamline. 1pC in 3D ellipsoid, Trms=1.8ps, transverse rms spot size =20um, Egun=60MV/m, phase on-crest, Eboo=0, B(T)=0.22T→ minimum emittance at EMSY1.

Conclusions and outlook

- Cigar beam mode in an S-band rf photoinjector was explored first time
- Transverse and longitudinal beam profiles were measured and found in good approximation to be parabolic, consistent of uniformly filled ellipsoidal distribution
- New measurement technique was discussed for ultralow emittance beams
- A new regime of rf photoinjector operation where the electron beam generated by a narrowly focused, longitudinally shaped laser pulse evolves into a nearly ideal uniformly filled 3D ellipsoid
- Initial transverse laser beam distribution used in experiment was in good approximation Gaussian for such very small spot size and nonlinear forces still have an impact on the emittance. Further improvements can be made to providing uniform, ultrasmall laser spot on the cathode

Literature

[1] I. V. Bazarov, B. M. Dunham, and C. K. Sinclair, Phys. Rev. Lett. **102**, 104801 (2009).

[2] X. J. Wang, Z. Wu, and H. Ihee, in *Proceedings of the 20th Particle Accelerator Conference, Portland, OR, 2003* (IEEE, New York, 2003), WOAC003.

[3] J. B. Hastings, F. M. Rudakov, D. H. Dowell, J. F. Schmerge, J. D. Cardoza, J. M. Castro, S. M. Gierman, H. Loos, and P. M. Weber, Appl. Phys. Lett. **89**, 184109 (2006).

[4] P. Musumeci, J. T. Moody, C. M. Scoby, M. S. Gutierrez, and M. Westfall, Appl. Phys. Lett. **97**, 063502 (2010).

[5] J. B. Rosenzweig *et al.*, Nucl. Instrum. Methods Phys. Res., Sect. A **593**, 39 (2008).

[6] S. Reiche, P. Musumeci, C. Pellegrini, and J. B. Rosenzweig, Nucl. Instrum. Methods Phys. Res., Sect. A **593**, 45 (2008).

[7] M. Boscolo, M. Ferrario, I. Boscolo, F. Castelli, S. Cialdi, V. Petrillo, R. Bonifacio, L. Palumbo, and L. Serafini, Nucl. Instrum. Methods Phys. Res., Sect. A **593**, 137 (2008).

[8] X. F. D. Stragier, O. J. Luiten, S. B. van der Geer, M. J. van der Wiel, and G. J. H. Brussaard, J. Appl. Phys. **110**, 024910 (2011).

[9] A. R. Rossi *et al.*, in *Proceedings of the 3rd International Particle Accelerator Conference, New Orleans, LA, 2012* (IEEE, New York, 2012), WEEPPB002.